[논 문] 한국재료학회지
Kor. J. Mater. Res.
Vol. 20, No. 1 (2010)

DOI: 10.3740/MRSK.2010.20.1.037

High Temperature Creep Behavior in Al-Mg(Zn)-Fe Alloys

Chang-Hwan Bae, Ju-Hee Lee and Chang-Suk Han*†

Dept. of Mechatronics Eng., Graduate School of M. T. &M., Hoseo University
*Dept. of Defense Science & Technology, Hoseo University 165 Sechul-Ri, Baebang-Myun, Asan City, Chungnam 336-795, KOREA

(Received November 13, 2009 : Received in revised form January 12, 2010 : Accepted January 12, 2010)

Abstract Creep tests were conducted under a condition of constant stress on two aluminum-based alloys containing particles: Al-5% Mg-0.25% Fe and Al-5% Zn-0.22% Fe. The role of grain boundary sliding was examined in the plane of the surface using a square grid printed on the surface by carbon deposition and perpendicular to the surface using two-beam interferometry. Estimates of the contribution of grain boundary sliding to the total strain, $\varepsilon_{gbs} / \varepsilon_t$ reveal two trends; (i) the sliding contribution is consistently higher in the Al-Mg-Fe alloy, and (ii) the sliding contribution is essentially independent of strain in the Al-Mg-Fe alloy, but it shows a significant decrease with increasing strain in the Al-Zn-Fe alloy. Sliding is inhibited by the presence of particles and its contributions to the total strain are low. This inhibition is attributed to the interaction between the grain boundary dislocations responsible for sliding and particles in the boundaries.

Key words aluminum-based alloys, grain boundary sliding, two-beam interferometry, total strain, constant stress, grain boundary dislocations.

1. Introduction

Grain boundary sliding is an important deformation mechanism in polycrystalline materials at elevated temperatures. Sliding occurs by the relative displacement of two adjacent grains, probably through the movement of grain boundary dislocations, and this displacement may be accommodated by intragranular slip throughout the grains, localized slip near the boundaries, the formation of triple point folds or the opening up of wedge cracks at the triple junctions or cavities at ledges and perturbations along the boundaries.[1-3)]

The process of sliding is illustrated schematically in Fig. 1. Two adjacent grains, designated 1 and 2, are displaced by sliding under an external applied stress σ. The sliding vector in the boundary plane, s, may be resolved into three mutually perpendicular components : u is the component measured along the tensile axis and w and v are the two components perpendicular to the tensile axis and either in the plane of or perpendicular to the specimen surface, respectively. Two angles, θ and ψ, define the trace of the boundary with respect to the tensile axis either on the surface or on a plane cut perpendicular to the surface and parallel to the tensile axis, respectively.

†Corresponding author
E-Mail : hancs@hoseo.edu (C. -S. Han)

Numerous experiments have been carried out to determine the strain contributed by grain boundary sliding, ε_{gbs}, to the total strain, ε_t, and, data are now available for a wide range of materials.[4)] However, only limited information is available on the role of grain boundary sliding in alloys where the boundaries contain particles.[5)] This paper summarizes some results obtained for grain boundary sliding in two aluminum-based alloys containing particles.

2. Experimental Procedure

Tests were conducted using two different aluminum alloys designated Al-5% Mg-0.25% Fe (P) and Al-5% Zn-0.22% Fe (P), respectively, where P denotes a pure grade of alloy. The measured impurity levels for these two alloys were 90 and 70 ppm, respectively. Each alloy was

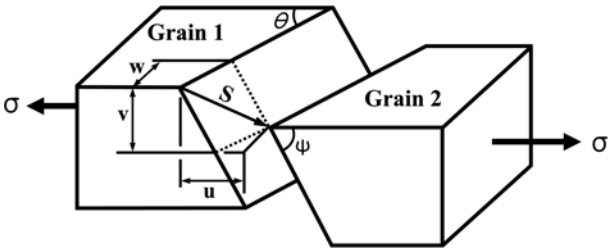

Fig. 1. Grain boundary sliding between grains 1 and 2 under an applied stress σ, showing the three components of sliding u, v and w.

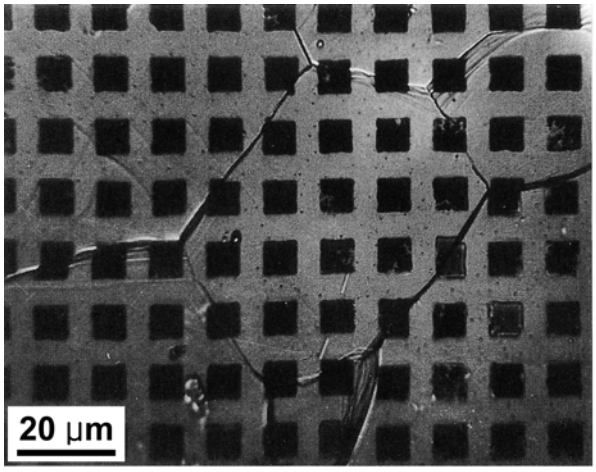

Fig. 2. The appearance of the printed grid on the Al-Mg-Fe alloy after testing to a strain of 0.068 at 623 K under a stress of 10.54 MPa.

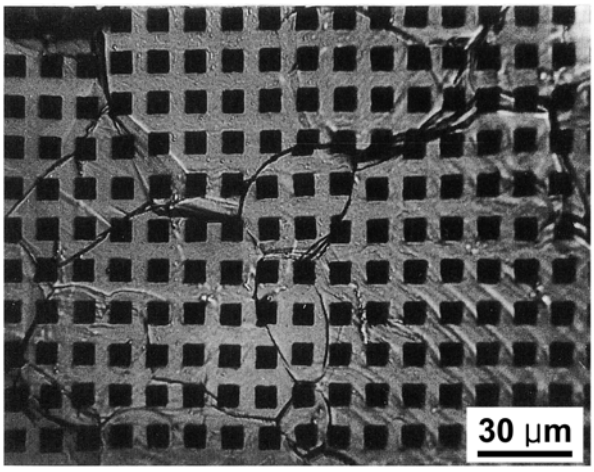

Fig. 3. The appearance of the printed grid on the Al-Mg-Fe alloy after testing to a strain of 0.203 at 623 K under a stress of 19.19 MPa.

supplied as hot-rolled sheet, with a thickness of 22 mm, and tensile specimens were cut parallel to the rolling direction. All specimens were annealed in air at 823 K prior to testing to produce grain sizes in the range of ~50-200 μm.

Creep tests were conducted under conditions of constant stress and each test was interrupted periodically in order to take measurements of the *v* offsets using interferometry. For some specimens, grids were printed onto the surfaces using a nickel stencil with square holes, 6.35 μm on each side and with a 6.35 μm separation, by exposing in a vacuum and depositing a layer of carbon.[6] The stencil was subsequently removed to permit observations of the occurrence of sliding in the plane of the surface during creep testing.

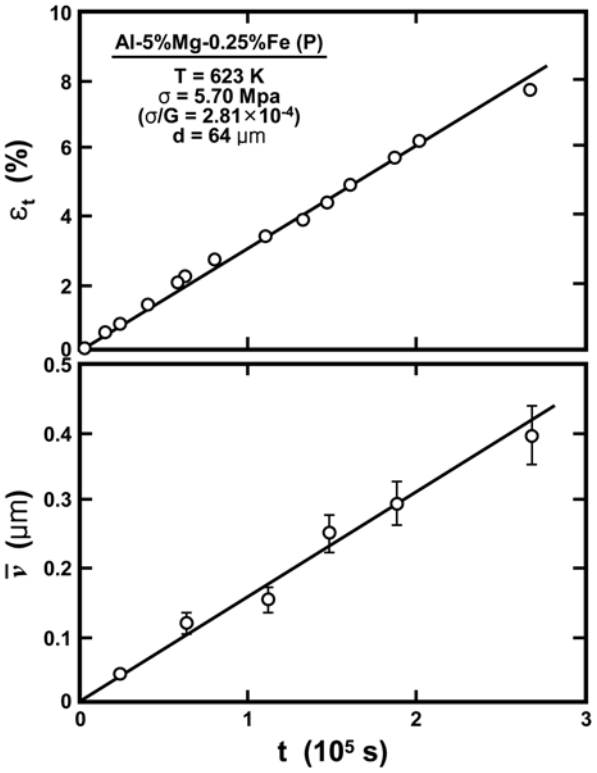

Fig. 4. Total strain ε_t (upper) and average grain boundary offset perpendicular to the surface $\bar{v}$ (lower) versus time for the Al-Mg-Fe alloy.

3. Results

Extensive grain boundary sliding occurred in both alloys when creep tested at high temperatures. Figs. 2 and 3 show examples of the appearance of the surface grid on the Al-Mg-Fe alloy after testing at 623 K under applied stresses of 10.54 and 19.19 MPa to total strains of 0.068 and 0.203, respectively. These two stress levels correspond to average strain rates of $\sim 2 \times 10^{-6}$ and $\sim 2 \times 10^{-5}\,s^{-1}$, respectively. In these two photomicrographs, the tensile axis is vertical and there is very clear evidence for grain boundary sliding along the boundaries lying at approximately 45° to the stress axis. There is also an absence of any significant triple point folding although these folds are a common feature of high temperature deformation in high purity Al.

Experiments of this type may be used to measure the *u* or *w* components of sliding in the plane of the surface but a more accurate procedure is to use two-beam interferometry to measure the *v* component.

Measurements were taken of the *v* component of sliding perpendicular to the surface at different increments of time for the two alloys. Figs. 4 and 5 show plots as a

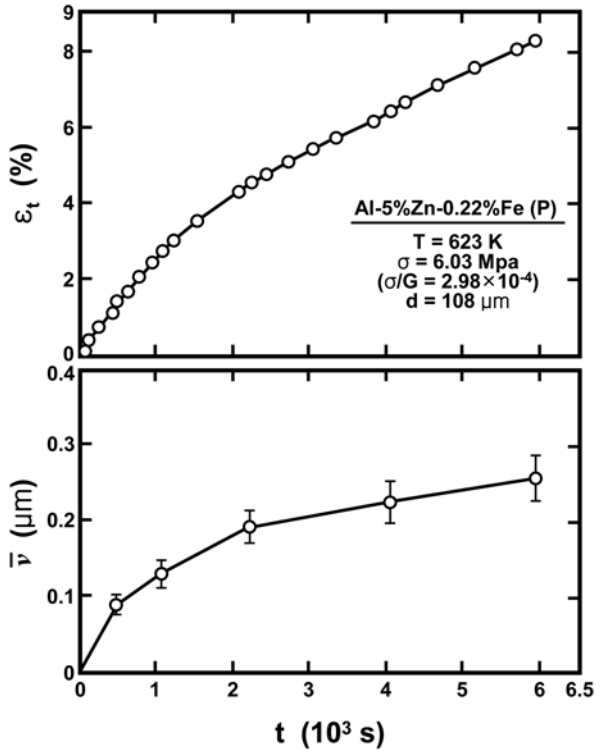

Fig. 5. Total strain ε_t (upper) and average grain boundary offset perpendicular to the surface $\bar{v}$ (lower) versus time for the Al-Zn-Fe alloy.

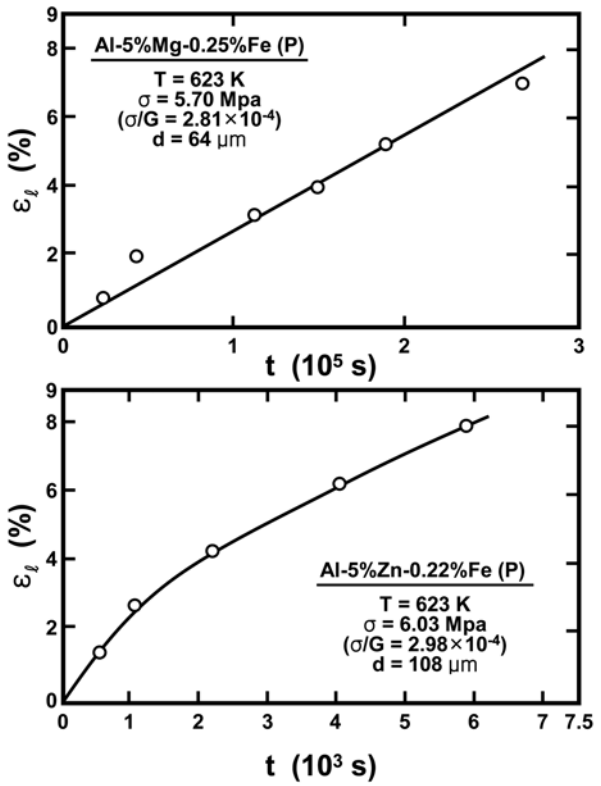

Fig. 6. Intragranular strain versus time for the Al-Mg-Fe (upper) and Al-Zn-Fe (lower) alloys, respectively.

function of time t of the total strain ε_t (upper) and the average value $\bar{v}$ determined from measurements of the v offsets at three hundred different boundaries (lower) for the Al-Mg-Fe and Al-Zn-Fe alloys, respectively. The error bars on the measurements of v represent the 95% confidence levels. Figs. 4 and 5 also include details of the applied stress, σ, the normalized stress, σ/G, where G is the shear modulus, and the specimen grain size, d.

These two plots show that the variation of $\bar{v}$ with time is similar to the variation with time of ε_t. In the Al-Mg-Fe alloy, ε_t and $\bar{v}$ both increase linearly with time so that, as observed also in the Al-5% Mg solid solution alloy under some testing conditions,[7] there is evidence for little or no primary creep. By contrast, the Al-Zn-Fe alloy shows a distinct primary stage where the creep rate decreases with increasing time and this trend is also reflected in the measurements of $\bar{v}$.

It is possible to use these sliding measurements to estimate the strain due to intragranular deformation, ε_l. Thus, taking ε_t at as the sum of the strain contributed by grain boundary sliding, ε_{gbs}, and the intragranular strain, ε_l, and defining ε_{gbs} as $\phi\ \bar{v}/d$ where ϕ is a constant of the order of unity, the experimental data of Figs. 4 and 5 may be replotted as ε_l versus t, as shown in Fig. 6. These two plots show that, for both alloys, the variation with time of ε_l is similar to that of ε_t and $\bar{v}$. Thus, the results serve to demonstrate that grain boundary sliding occurs in an analogous manner to, and has an interconnection with, the intragranular deformation. The conclusion of a relationship between sliding and deformation within the grains was first suggested in very early experiments on grain boundary sliding using simple polycrystalline materials such as Al,[8] Al alloys[9] and Pb[10] and the trend is now further established for alloys containing particles.

In order to make a direct comparison between the magnitudes of sliding in the two alloys under similar testing conditions, Fig. 7 gives a plot of $\bar{v}$ versus ε_t for the Al-Mg-Fe and Al-Zn-Fe alloys at the same testing temperature and at very similar values of σ/G. It should be noted, however, that the grain sizes of the two alloys are 64 and 108 μm, respectively. An examination of Fig. 7 shows that the initial values of $\bar{v}$ are very similar but larger sliding offsets are recorded in the Al-Mg-Fe alloy at strains above ~4%.

The experimental data in Fig. 7 can be used to estimate the contribution of grain boundary sliding to the total

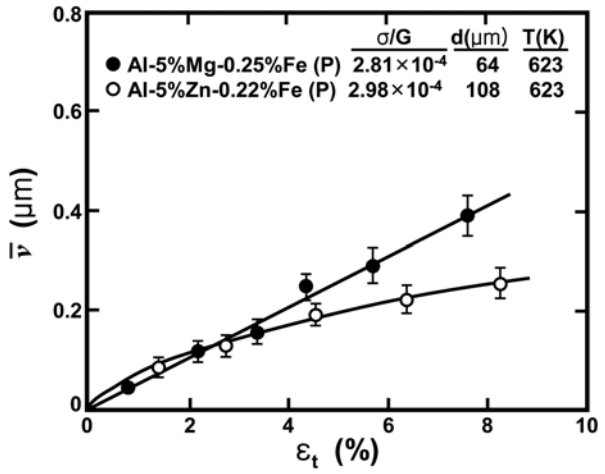

Fig. 7. Values of $\bar{v}$ versus ε_t for the two alloys tested at the same temperature and at similar values of σ/G.

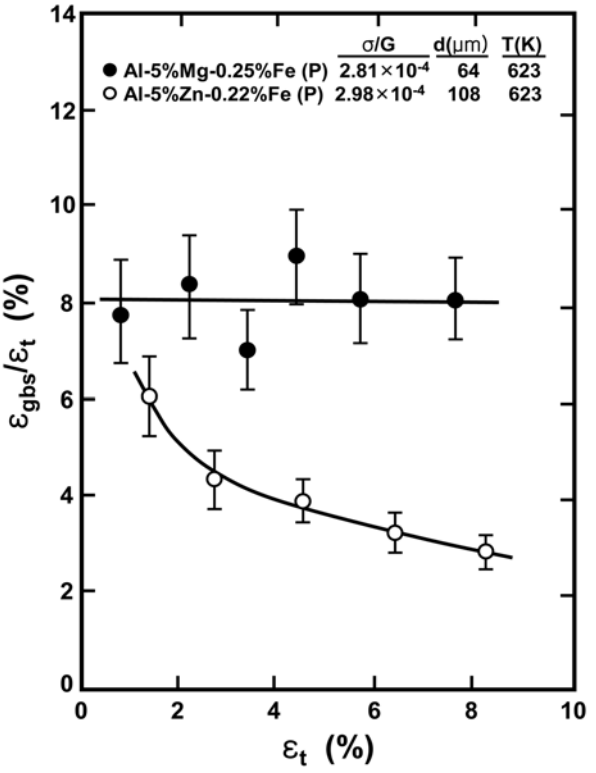

Fig. 8. Contribution from grain boundary sliding to the total strain in the Al-Mg-Fe and Al-Zn-Fe alloys.

strain, $\varepsilon_{gbs} / \varepsilon_t$. The result is shown in Fig. 8 where $\varepsilon_{gbs} / \varepsilon_t$ is plotted as a function of ε_t for the two alloys. These results reveal two important trends.

First, the sliding contribution is consistently higher in the Al-Mg-Fe alloy. Second, the sliding contribution is essentially independent of strain in the Al-Mg-Fe alloy but the contribution shows a significant decrease with increasing strain in the Al-Zn-Fe alloy. It is important to

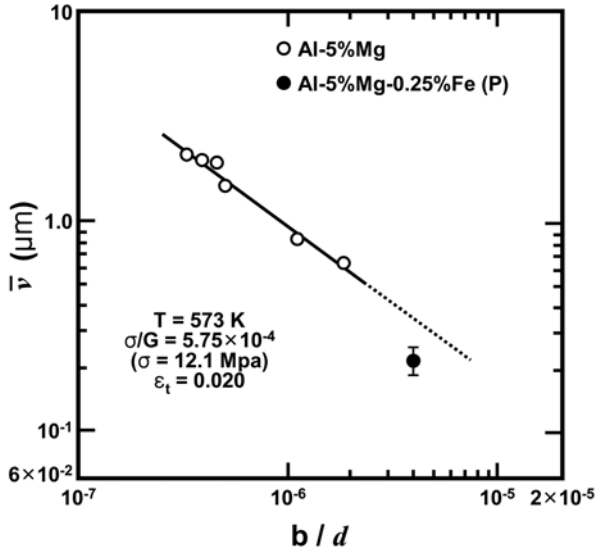

Fig. 9. Average grain boundary offset perpendicular to the surface $\bar{v}$ versus the normalized inverse grain size b/*d* for the Al-Mg-Fe alloy and an Al-5% Mg solid solution alloy.

note, however, that the total sliding contributions are very low, and under a value of 10%, in both alloys under the present experimental conditions.

It is possible to examine the effect of particles on the extent of grain boundary sliding by making a direct comparison with a solid solution alloy where no particles are present. Fig. 9 shows a plot of $\bar{v}$ versus the normalized inverse grain size, b/*d*, where b is the Burgers vector; the datum points for the Al-5% Mg solid solution alloy were taken from the experiments of Vetrano[7] and the single point for the Al-Mg-Fe alloy was obtained in the present investigation. For all of the datum points in Fig. 9, the tests were conducted at a stress of 12.1 MPa, equivalent to $\sigma/G = 5.75 \times 10^{-4}$, a testing temperature of 573 K, and all of the values of $\bar{v}$ relate to a total strain of $\varepsilon_t = 0.02$. It is clear from Fig. 9 that, even when considering the error bars on the $\bar{v}$ measurements, the presence of particles inhibits the rate of grain boundary sliding. Thus, it is reasonable to anticipate smaller sliding offsets in alloys where particles are located on the grain boundaries and therefore relatively lower values for the sliding contribution $\varepsilon_{gbs} / \varepsilon_t$.

4. Discussion

Grain boundary sliding is an important deformation mechanism in polycrystalline materials subjected to high temperature creep but the extent of sliding depends both

upon the experimental testing conditions and the nature of the grain boundaries. When particles are present at the boundaries, as in the Al-Mg-Fe and Al-Zn-Fe alloys, grain boundary sliding tends to be inhibited and the sliding contributions to the total strain are rather low.

From experiments on Al-0.05% Fe bicrystals, Horton[11] suggested that the reduction in sliding in the presence of particles may be due to three possible mechanisms: (i) an inhibition of grain boundary migration due to the particles, (ii) the role of plastic accommodation around each particle, or (iii) an interaction between the grain boundary dislocations responsible for sliding and the particles lying in the grain boundaries. Of these three possibilities, Fig. 2 shows that grain boundary migration is not inhibited, and the third explanation appears probable because there is extensive evidence for the movement of grain boundary dislocations during high temperature deformation.[12]

Finally, Fig. 8 shows that sliding tends to be of greater significance in the Al-Mg-Fe alloy than in the Al-Zn-Fe alloy. This difference may arise in part because the movement of grain boundary dislocations is more retarded by the drag force due to the Mg solute atoms than the Zn solute atoms and in part because extrinsic dislocations enter the grain boundaries from the lattice and the intragranular dislocation distribution is relatively uniform in Al-5% Mg whereas it is inhomogeneous in Al-5% Zn.[13] The latter effect probably leads to a larger concentration of mobile extrinsic grain boundary dislocations in the Al-Mg-Fe alloy and therefore a higher contribution from sliding to the total strain.

5. Conclusion

The results of this investigation are summarized below.

1. In the Al-Mg-Fe alloy, ε_t and $\bar{v}$ both increase linearly with time, by contrast, the Al-Zn-Fe alloy reveals a distinct primary stage where the creep rate decreases with increasing time and this trend is reflected also in the measurements of $\bar{v}$.

2. The estimate the contribution of grain boundary sliding to the total strain, ε_{gbs} / ε_t reveal two trends; (i) the sliding contribution is consistently higher in the Al-Mg-Fe alloy, and (ii) the sliding contribution is essentially independent of strain in the Al-Mg-Fe alloy but the contribution shows a significant decrease with increasing strain in the Al-Zn-Fe alloy.

3. Sliding is inhibited by the presence of particles and the contributions from sliding to the total strain are low. This inhibition is attributed to the interaction between the grain boundary dislocations responsible for sliding and particles lying in the boundaries.

References

1. O. A. Ruano, J. Wadsworth and O. D. Sherby, Acta Mater., **51,** 3617 (2003).
2. H. Muto and M. Sakai, Acta Mater., **48,** 4161 (2000).
3. S. B. Biner, Acta Mater., **44,** 1813 (1996).
4. D. H. Zeuch, Mechanics of materials, **3,** 111 (1984).
5. J. Cadek, Acta Techn. CSAV, **37,** 13 (1992).
6. J. D. Parker and B. Wilshire, Mater. Sci. Eng., **29,** 219 (1977).
7. J. S. Vetrano, E. P. Simonen and S. M. Bruemmer, Acta Mater., **47,** 4125 (1999).
8. D. McLean and M. H. Farmer, J. Inst. Metals, **85,** 41 (1957).
9. D. McLean and M. H. Farmer, J. Inst. Metals, **83,** 1 (1955).
10. R. C. Gifkins, J. Austral. Inst. Metals, **8,** 148 (1963).
11. C. A. P. Horton, Acta Met., **20,** 477 (1972).
12. P. R. Howell, J. O. Nilsson, A. Horsewell and G. L. Dunlop, J. Mater. Sci., **16**, 2860 (1981).
13. M. T. Perez-Prado, M. C. Cristina and O. A. Ruano, Mater. Sci. Eng. A, **244,** 216 (1998).